Hindawi
International Journal of Antennas and Propagation
Volume 2019, Article ID 3782528, 10 pages
https://doi.org/10.1155/2019/3782528

Research Article

A Compact 5G Decoupling MIMO Antenna Based on Split-Ring Resonators

Ziyu Xu, Qisheng Zhang, and Linyan Guo

School of Geophysics and Information Technology, China University of Geosciences, Beijing, China

Correspondence should be addressed to Linyan Guo; guoly@cugb.edu.cn

Received 28 February 2019; Revised 18 April 2019; Accepted 28 April 2019; Published 2 June 2019

Guest Editor: Sreedevi Menon

A compact planar multiple-input multiple-output (MIMO) antenna array for 5G band is proposed in this paper. To improve the isolation of compact microstrip antenna array, this paper mainly presents an electromagnetic resonant ring method for MIMO antenna array. The proposed antenna can cover both the 3.3-3.6 GHz and 4.8-5 GHz bands proposed for the 5G band. The antenna proposed in this paper consists of two symmetrical meandered monopole radiators, grid structures, and a Y-shape element. Two different sizes of split-ring resonators (SRRs) are used to suppress the interference of the coupled signal to the antenna system; thereby it can reduce the mutual coupling effect. The experimental results show that the mutual coupling between the two elements is below -25 dB in both of the bands after adding the SRRs. And this antenna is only 23×19 mm^2. Its compact size and structure can be used as a mobile terminal antenna.

1. Introduction

With the rapid development of wireless communication technology, mobile communication has been integrated into all aspects of life. Nowadays, fifth generation is becoming a hot spot in the field of global research because of its faster transmission rate and higher performance [1]. At present, the fifth generation of mobile communications (5G) of the band is identified as two frequency bands in 3.3-3.6 GHz and 4.8-5 GHz. Total of 500 MHz bandwidth of these frequencies can be reached. And in communication systems, multiple-input multiple-output (MIMO) techniques can significantly improve spectrum utilization and channel capacity without increasing transmit power and adding additional transmission bandwidth [2, 3]. However, as the miniaturization and portability of wireless devices become mainstream, the available space for antennas is more limited. Therefore, it is very necessary to design a compact MIMO antenna. In order to adapt to the commonly used wireless devices, printing MIMO antennas is a necessary choice. However, there is strong mutual coupling when the distance between MIMO antenna elements is very close. It is contrary to the desire for higher isolation and lower envelope correlation coefficients. Hence, it is indispensable to reduce the mutual coupling between the antenna elements.

From the existing literatures, the researchers have done a lot of work in reducing coupling and have proposed various solutions. In order to suppress the propagation of surface waves and reduce the coupling, a parasitic branching method [4] can usually be used. There are also many methods for improving the electromagnetic wave propagation in a certain frequency band by using an electromagnetic band gap structure [5, 6]; they can form a frequency band gap and a phase band gap characteristic to improve isolation. Changing the current propagation path to restrain coupling multiple often chooses neutralization line techniques [7, 8]. Besides, it is also common to use a defective ground structure [9–11] as a band-stop filter to achieve decoupling. In addition to the traditional methods, the method of using the special properties of metamaterials to achieve the desired effect is also mentioned in [12–14]. But the above-mentioned methods are having insufficient space on a compact MIMO antenna and are difficult to function. Therefore, this paper proposes to reduce the coupling by using two different sizes of split-ring resonators (SRRs).

This paper presents a compact binary array printed MIMO antenna. The antenna can cover the 5G band recently proposed by the Ministry of Industry and Information Technology of China. The proposed antenna has a symmetrical structure. And it uses microstrip feed line. In this paper,

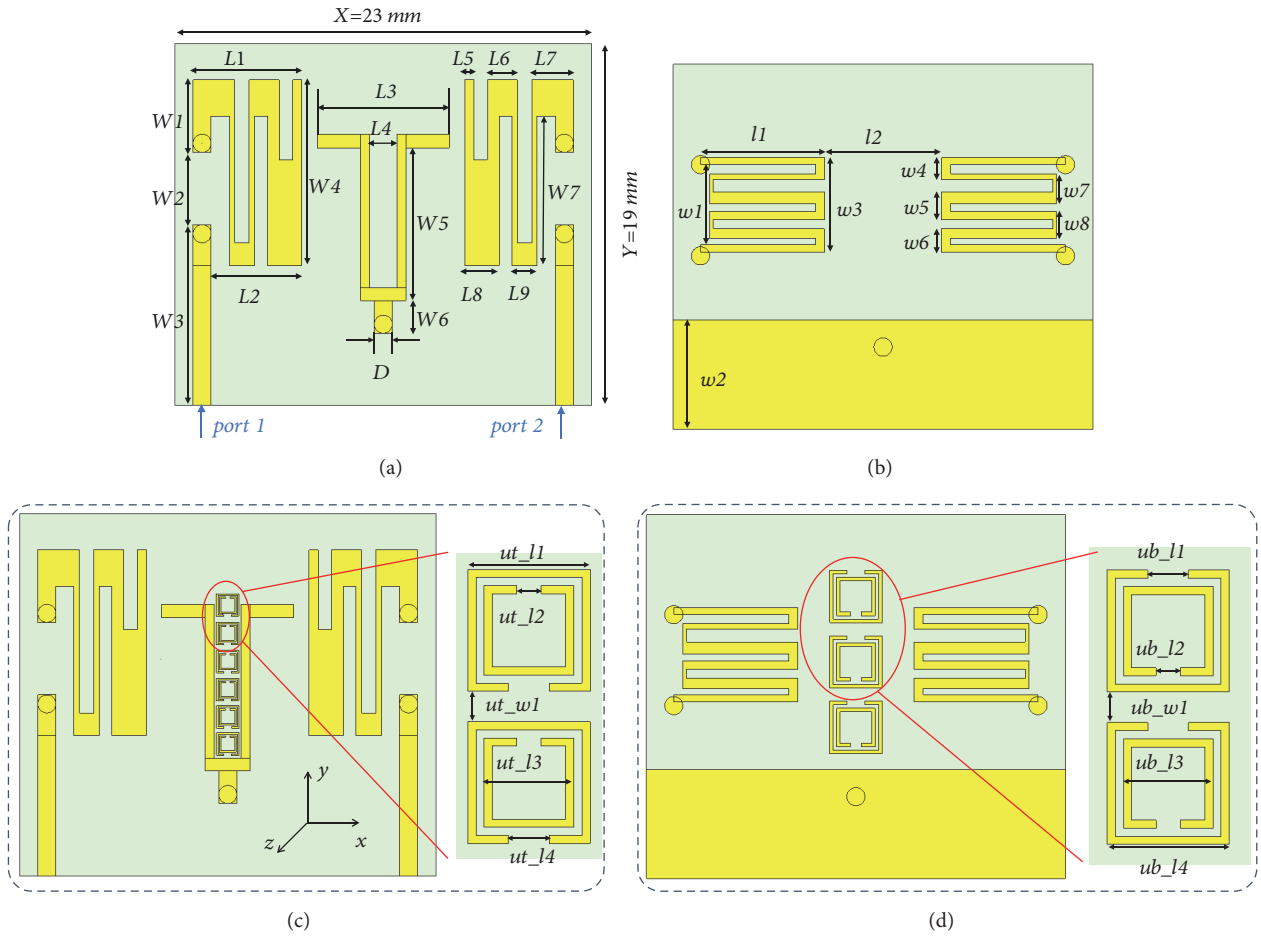

FIGURE 1: (a) The top of the antenna without SRRs. (b) The bottom of the antenna without SRRs. (c) The top of the antenna with SRRs. (d) The bottom of the antenna with SRRs.

electromagnetic waves resonate when they arrive at the SRRs, thereby effectively impeding the propagation of the electromagnetic wave and reducing the mutual coupling between the two antenna elements. The second part introduces the specific structure and size of the antenna. The third part gives the detail of simulated and measured results of the antenna. At the same time, the performance of the antenna and decoupling structure are analyzed and discussed in this section. Finally, the proposed MIMO antenna is summarized.

2. Antenna Design

The proposed antenna is printed on the Rogers 4003C substrate of thickness 0.406 mm with a dielectric constant of 3.38 and loss tangent of 0.0027. The size is only 23×19 mm^2, which is considered compact enough. The metal here is a 0.035 mm thickness copper with a conductivity of 5.8 × 10^7 S/m. The simulated model of the proposed MIMO antenna is shown in Figure 1. This antenna uses the microstrip feed line method. It can be seen from the front view (shows in the Figure 1(a)) that the proposed MIMO antenna is consisted of two monopole radiators and a Y-shape connected to the ground through metal via hole. And the bottom of the antenna constitutes ground and two meandered lines strips connected to the respective radiators, which are connected to the radiators through metal via holes as shown in the Figure 1(b).

In the MIMO antenna model proposed in this paper, the resonant frequency and the resonant intensity are mainly determined by the parameters of each structure. Different structures and shapes can form different electrical lengths, resulting in different resonant frequencies. The right side of the monopole radiation element at the top of the dielectric slab and the corresponding bend line at the back mainly affect the frequency of 4.9 GHz. The length of the short side of the Y-shaped structure plays a major role at the resonant frequency of 3.52 GHz. By analyzing the structure that affects the resonant frequency, the size of the structure can be adjusted to achieve the change of the resonant frequency.

Although the coverage of the required frequency band can be achieved, the antenna distance is very close, only $0.18\lambda_{5G}$; the two array elements have highly coupled. It is a common problem in MIMO applications. Therefore, in order to reduce the mutual coupling between the antenna elements and improve the isolation, the decoupling structures shown in Figures 1(c) and 1(d) are added. Figure 1(c) illustrates that six smaller SRRs are added to the front of the antenna. In Figure 1(d), three larger SRRs are added to the bottom

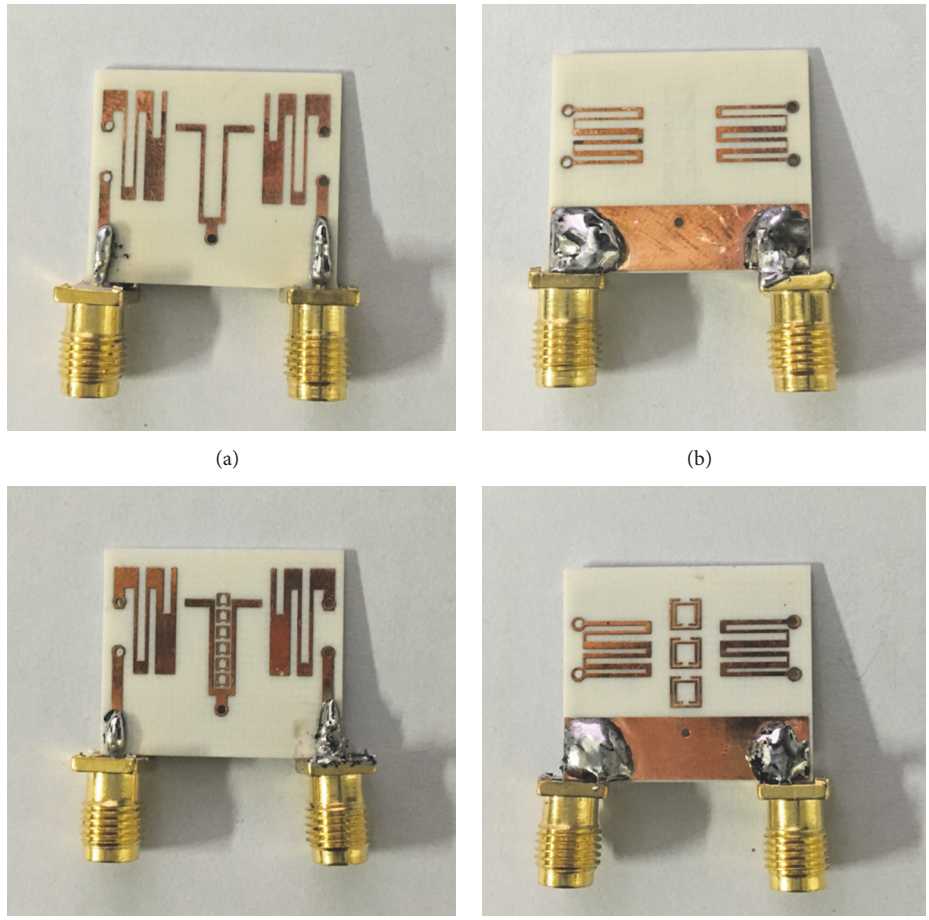

Figure 2: Fabricated prototype of the MIMO antennas. (a) The top of original antenna, (b) the bottom of original antenna, (c) the top of the decoupling antenna, and (d) the bottom of the decoupling antenna.

of the antenna. Considering several situations, we finally chose to place SRRs on both sides. The combination of these decoupling structures can well restrain the mutual coupling at the bands of 3.52 GHz and 4.9 GHz.

The specific size and distance of each structure are finally determined by electromagnetic simulation software CST Microwave Studio, as shown in Table 1. In order to have a good impedance matching with a 50-Ω standard SMA connector, the width of the feed line is designed to be 1 mm.

3. Simulation and Experimental Results

In this section, we will discuss the antennas' simulated and measured results. To verify the simulation, a prototype of the proposed antenna is constructed and measured based on the design and dimensions thereof described in Figure 1. Due to limitations of the manufacture technology, the metal via hole embedded into the dielectric are fabricated as electroplated with a channel diameter of 0.05 mm. The experimental test in this paper uses a vector network analyzer (Agilent E8362B). In experimental measurements, the proposed MIMO antenna is fabricated on a 0.406 mm thick Rogers 4003C substrate. The deposited copper thickness was 0.035 mm. The photograph of the fabricated antenna prototype is shown in Figure 2. The top and the bottom of original antenna are given in Figures 2(a) and 2(b), and Figures 2(c) and 2(d) show the top and bottom of decoupling antenna, respectively. It can be intuitively seen that this MIMO antenna is compact from the fabricated antenna.

3.1. S-Parameters. The simulated and measured S-parameters of the proposed MIMO antenna are sketched in Figures 3(a) and 3(b), respectively. During the test, the two ports of the antenna are, respectively, connected to the two ports of the vector network analyzer Agilent E8362B. Comparing Figures 3(a) and 3(b); the overall trend of the measured results is consistent with the simulated results, but there is a slight deviation. That is, the resonance points obtained by the test are all biased to the high frequency. It may be due to the frequency limit of the SMA connectors and the printed circuit board manufacture tolerance.

It can be noted from the S-parameters shown in Figure 3 that the proposed antenna has a good effect in the above-mentioned frequency bands. Each antenna can cover two frequency bands of 5G, and its return loss S11 can basically reach below -10 dB. With the addition of SRRs, the isolation

Table 1: The specific parameters of MIMO antenna.

parameters	mm	parameters	mm	parameters	mm
L1	6	*W5*	8.45	*w8*	1.5
L2	5	*W6*	2.5	*ut_l1*	1.244
L3	7.3	*W7*	8.25	*ut_l2*	0.249
L4	1.5	*D*	1	*ut_l3*	0.912
L5	0.5	*l1*	6.8	*ut_l4*	0.415
L6	1.65	*l2*	6.4	*ut_w1*	0.311
L7	2.3	*w1*	4.8	*ub_l1*	0.96
L8	1.9	*w2*	6	*ub_l2*	0.576
L9	1.4	*w3*	5.2	*ub_l3*	2.112
W1	4	*w4*	1.2	*ub_l4*	2.88
W2	4	*w5*	1.5	*ub_w1*	0.72
W3	10	*w6*	1.3		
W4	10.25	*w7*	1.65		

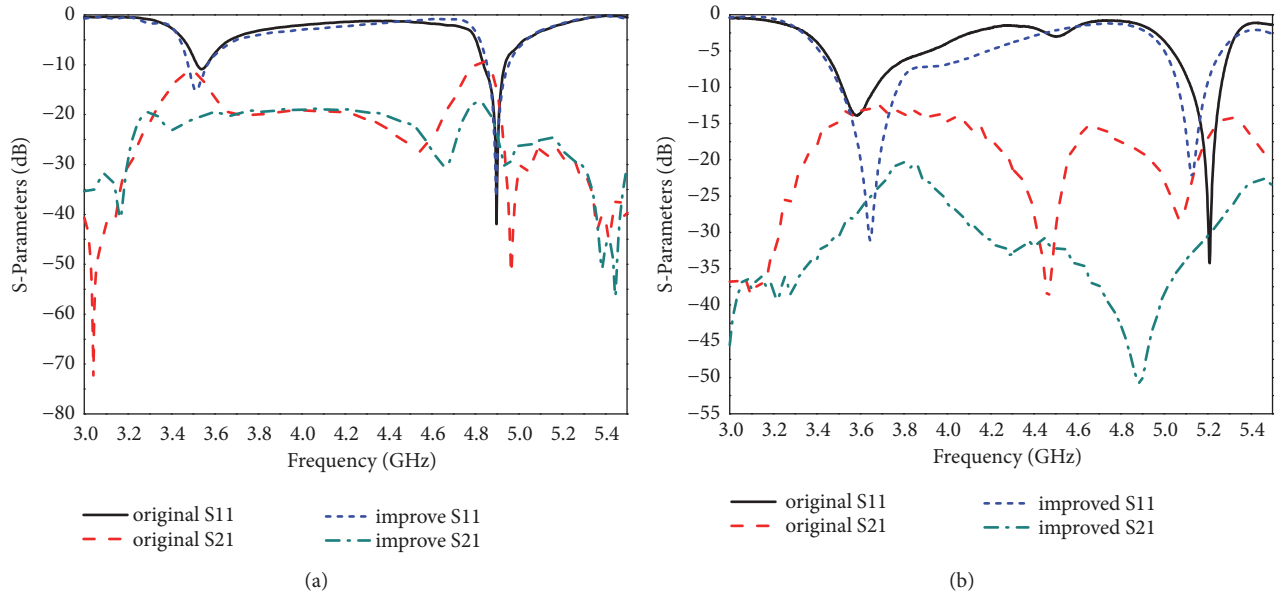

Figure 3: (a) Simulated S-parameters. (b) Measured S-parameters.

of all corresponding bands is better than 25 dB, improving about 10 dB. At the same time, the resonant frequency of the antenna is substantially not offset. The return loss at 3.52 GHz is also slightly better than the original antenna. It can be noticed from the return loss and isolation that the MIMO antenna proposed in this paper performs well. In the measured results, the centre frequency is slightly shifted to the high frequency due to factors such as dielectric plate loss and test feeder loss. There are some errors between the measured results and the simulated results. This may be the reason for the compact size of the antenna and the workmanship is imprecise. However, after adding the SRRs, the overall performance of the antenna is better than the original one.

The original antenna we designed in this paper has a Y-shape structure in the middle of the two radiation elements. The Y-shape structure in this design mainly serves to enhance the radiation effect of the resonant point. When there is no Y-shape structure, although S21 is lower than S11 at the resonance point, it is apparent that S11 at the resonance frequency is less than -10 dB, as shown in Figure 4. S11 with/without Y-shape structure is plotted in Figure 4(a). And Figure 4(b) shows the curves of S21 with/without Y-shape structure. Comparing the red solid line and the black dash line in Figure 4(a), the resonance of antenna is significantly enhanced in the desired frequency bands after adding the Y-shape structure, and the design requirements are met.

Normally, the ground plane will also participate in the radiation of the antenna, so its size will also affect the S-parameters. Using the control variable method, the other parts remain the same size, only the width of the ground plane is changed (the size of *w2*), as shown in Figure 5. It can be known from the figure that the resonant frequency will shift to the high frequency as the width of the ground plane increases, both in the low frequency and in the high frequency bands. When *w2*=5 mm, the performance of S11 is best in the 3.3-3.6 GHz band, but the S11 in the

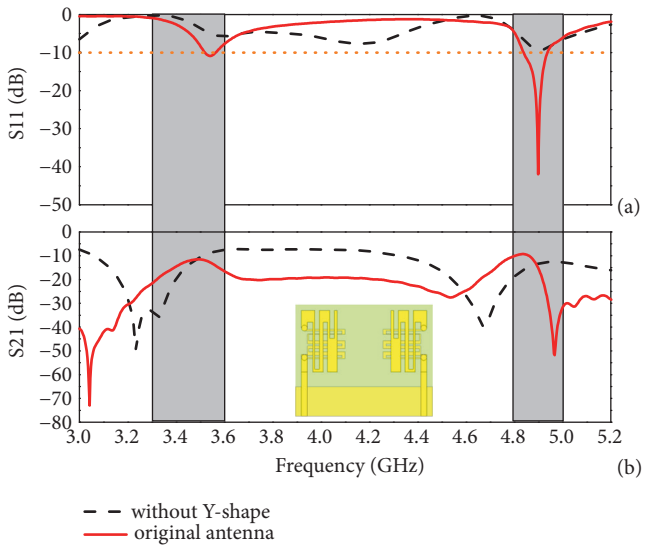

Figure 4: S-parameters with/without Y-shape structure: (a) S11 and (b) S21. Inset: Model of antenna without Y-shape structure.

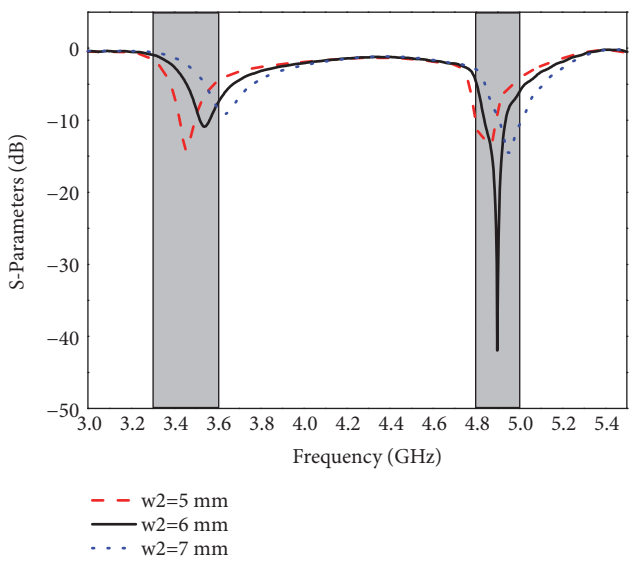

Figure 5: S-parameters of ground plane with different widths.

4.8-5 GHz band is slightly smaller and more biased towards low frequencies. When *w2*=7 mm, it has a slightly higher frequency in the 4.8-5 GHz band and S11 is slightly smaller, but its resonant frequency is already higher than 3.6 GHz in the band of 3.3-3.6 GHz and does not meet the < -10 dB requirement. Therefore, considering the comprehensive consideration, it is finally determined that the width of the ground plane is 6 mm.

Since the SRR can be equivalent to an *LC* series resonant circuit, its resonant frequency can be obtained substantially by $f_0 = 1/2\pi\sqrt{LC}$. L is the full inductance of the SRR. When calculating the SRR's inductance, it can be equivalent to a full-closed loop inductance. The split of the two rings can be equivalent to the capacitance C, which is the full capacitance of the SRR. The initial size of the SRR is obtained

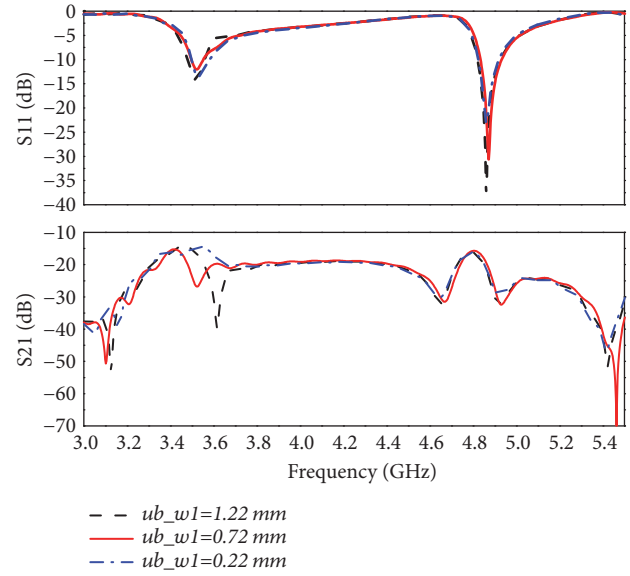

Figure 6: S-parameters of different distance between larger SRRs.

according to the formula mention above and then optimized by using CST Microwave Studio to obtain the final size. Take the distance between the larger SRRs on the bottom of antenna (the size of *ub_w1*) as an example for discussion. The S-parameter when *ub_w1* is changed can be seen from Figure 6. The change of *ub_w1* has little effect on S11, but it has a significant impact on S21. When *ub_w1*=1.22 mm, the frequency of coupling reduction at 3.52 GHz shifts to higher frequency. When *ub_w1*=0.22 mm, the decoupling effect is not significant at 3.52 GHz. Therefore, *ub_w1*=0.72 mm is the most ideal choice.

3.2. Radiation Patterns. To further validate the influence of the SRRs in the MIMO antenna, simulated and measured radiation patterns are plotted in Figures 7 and 8, respectively. Due to the symmetry of the antenna design, the antenna pattern shows good complementarity and orthogonality (the antenna's maximum radiating area is complementary and the main lobe is orthogonal). Therefore, only given the case when port 1 is fed, and port 2 is symmetric with it, the E planes (*yOz*) and H planes (*xOz*) at the two resonance points when port 1 is excited are shown in the figures. Among these, Figures 7(a) and 7(b) show the simulated E planes and H planes at 3.52 GHz. Figures 8(a) and 8(b) are the measured results at 3.52 GHz. And the E planes of the simulated and measured at 4.9 GHz are drawn in Figures 7(c) and 8(c). Figures 7(d) and 8(d) describe the simulated and measured results of the H plane at 4.9 GHz. In these figures, original antenna is drawn with black solid lines, and the improved antenna is drawn with red dashed lines. During the measurement, one port is excited and the other port is connected to the 50-Ω load. From the given results, the radiation omnidirectionality of the antenna is well. The observed radiation patterns show a good agreement with the simulated results and the measured results. Some differences here are possibly due to the factor that the test environment is nonanechoic chamber. It is evident from the

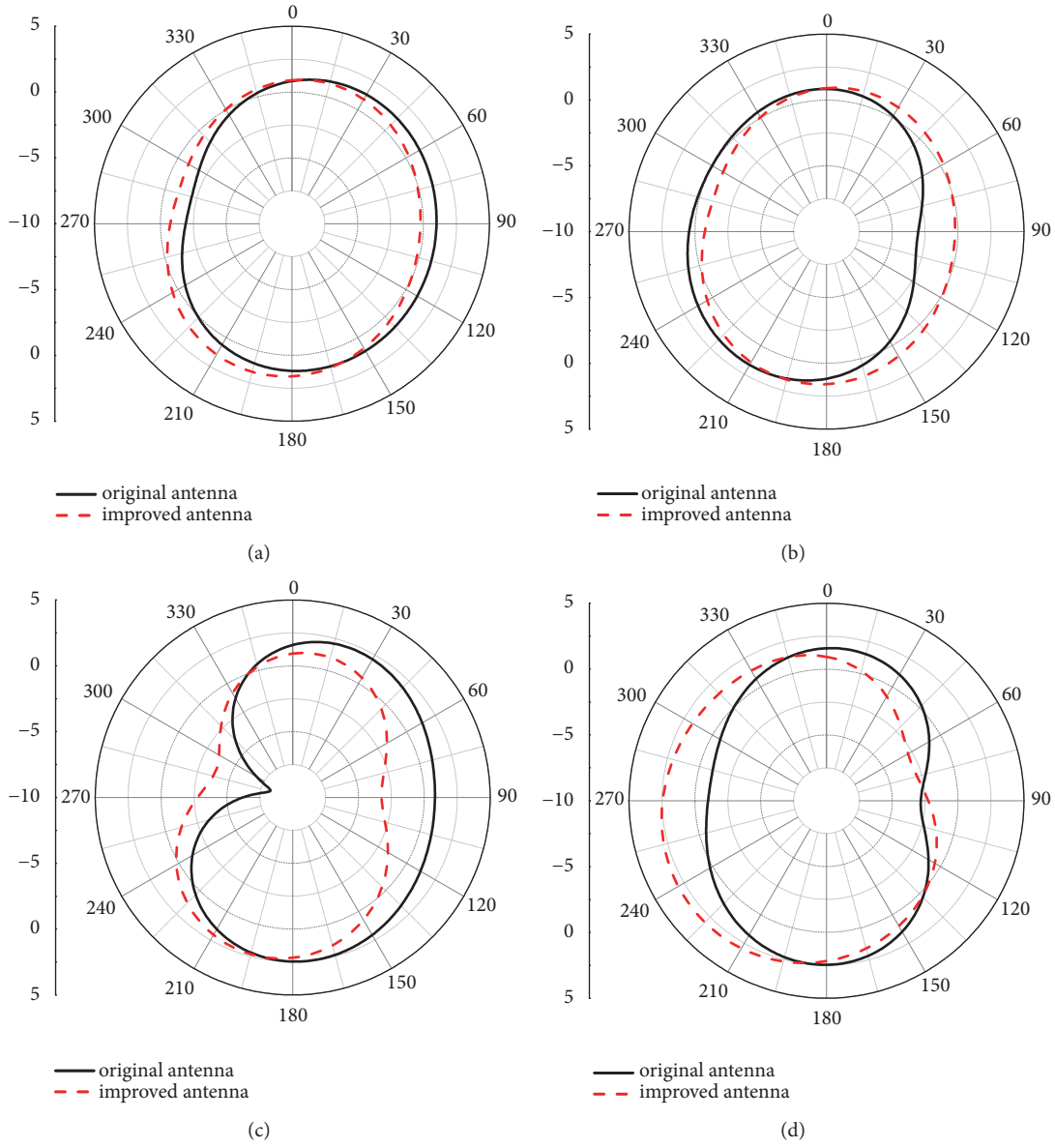

Figure 7: Simulated radiation pattern. (a) E plane and (b) H plane at 3.52 GHz; (c) E plane and (d) H plane at 4.9 GHz.

figures that loading the SRRs has little notable effect on radiation performance of the antenna. A slight inconsistency did not worsen the radiation performance of the antenna. The overall radiation performances of the antenna, such as gain and efficiency, are consistent with the original one.

3.3. Surface Current. In order to study the mutual coupling between the two antenna elements more intuitively and analyze the working mechanism of the SRRs at great length, the simulated results of CST are used to observe the surface current distribution of the antenna. Through these results, the influence of the SRRs on the MIMO antenna is discussed. In this paper, the decoupling structure is mainly composed of two different sizes of SRRs on the front and back sides. The surface current distribution of the antenna with or without SRRs at the excitation of port 1 at 3.52 GHz and 4.9 GHz is displayed in Figure 9. By comparing Figures 9(a) and 9(b), it can be seen that after SRRs are added, most of the current is concentrated to the SRRs on the back side, so that less current can reach the side of port 2, thus effectively reducing the mutual coupling. From the comparison of Figures 9(c) and 9(d), it can be concluded that the original antenna is without SRRs; the current can flow unimpeded to the side of port 2, and thus it has a high coupling. After loading the SRRs; the current propagation is limited, and the port 2 and the radiation of the right side cannot be reached directly, so the mutual coupling is suppressed. Therefore, introducing SRRs can reduce the coupling current of the nonexcited antenna elements. This is because when the coupling current passes through the metal resonant ring, it can effectively restrain the current radiated to the nonexcited antenna element, thereby improving the mutual coupling. For achieving the optimal decoupling effect, the size and position of the SRRs are determined through multiple simulations and optimizations.

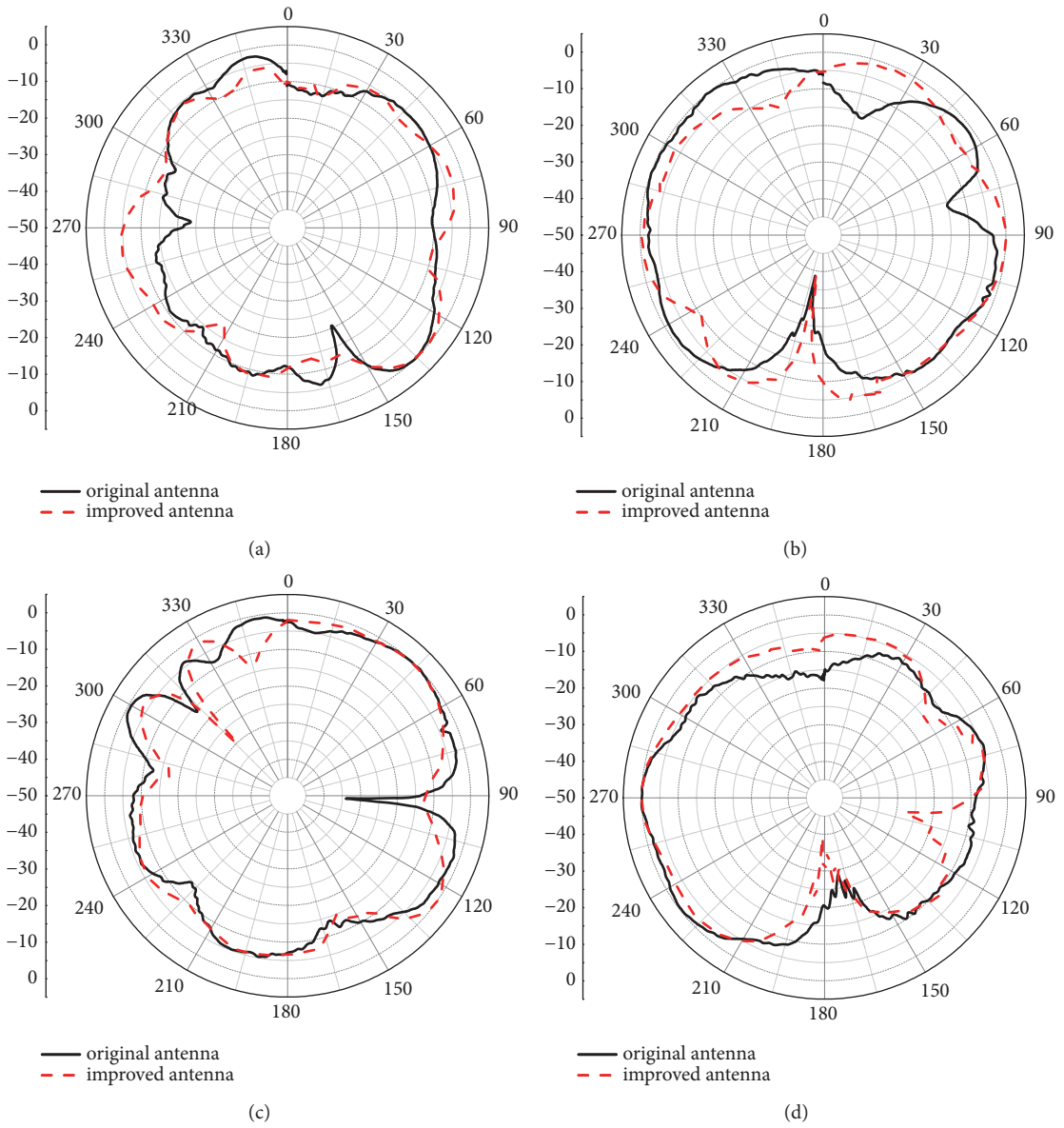

Figure 8: Measured radiation pattern. (a) E plane and (b) H plane at 3.52 GHz; (c) E plane and (d) H plane at 4.9 GHz.

From the simulated results and the measured results, the proposed decoupling structure has a good effect, which provides a thought for MIMO antenna decoupling and has a certain prospect.

3.4. ECC. The envelop correlation coefficient (ECC) is an important figure of merit for any MIMO enabled antenna systems. It can be calculated from the S-parameters of the antenna [15], as formula (1). In formula (1), S_{11}^* and S_{21}^* represent the conjugates of S11 and S21, respectively. The calculated ECC less than 0.5 is the most basic requirement for MIMO antenna. A comparison of ECC computed from S-parameters for MIMO antenna with and without SRRs is exhibited in Figure 10. It is clear that after adding the SRRs, ECC of the antenna is significantly reduced and is less than 0.3 in the required operating frequency band. That means the antenna with SRRs ensures good diversity performance.

$$\rho = \frac{\left|S_{11}^* S_{12} + S_{21}^* S_{22}\right|^2}{\left(1 - \left(\left|S_{11}\right|^2 + \left|S_{21}\right|^2\right)\right)\left(1 - \left(\left|S_{22}\right|^2 + \left|S_{12}\right|^2\right)\right)} \quad (1)$$

Furthermore, in order to distinguish our results from other existing equivalent antennas, the properties of the geometrical dimensions, the relationship between wavelength and size, type of substrate, the decoupling method, and other properties are compared in Table 2. In Table 2, λ represents the dielectric wavelength at the high frequency resonance point of the antenna. The maximum size of the antenna can be obtained by the relationship between λ and size. It is evidently illustrated from the table that the proposed MIMO antenna

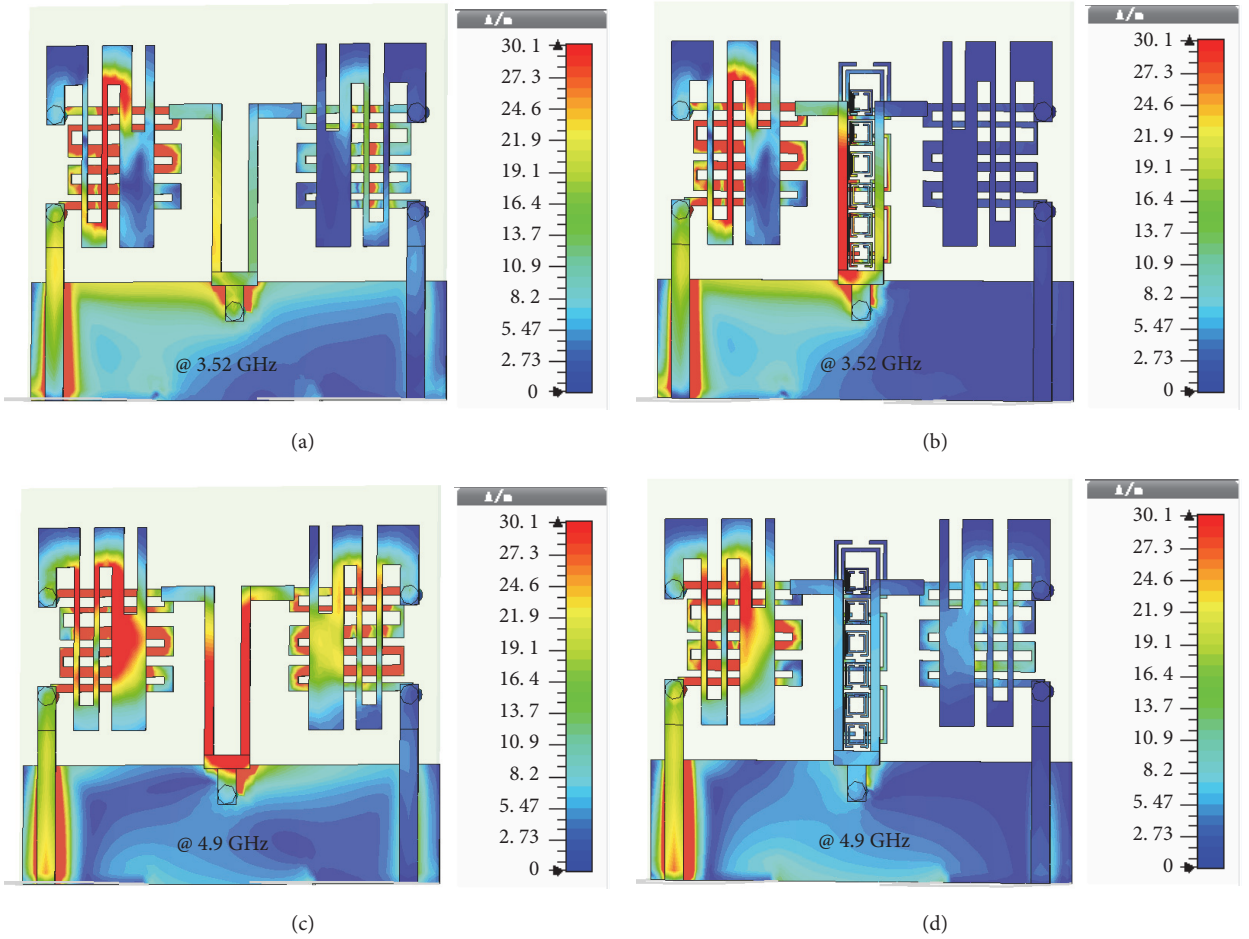

Figure 9: Surface current. (a) Original antenna and (b) improved antenna at 3.52 GHz; (c) original antenna and (d) improved antenna at 4.9 GHz.

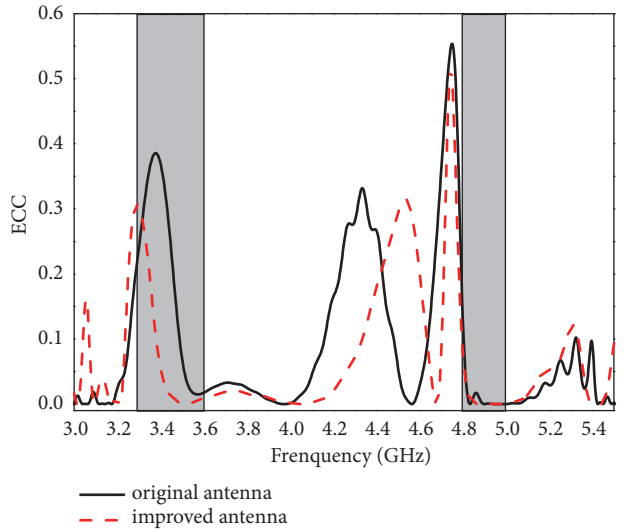

Figure 10: Envelop correlation coefficient.

Table 2: Comparison of proposed antenna and previous equivalent antennas.

	Geometrical dimensions (mm^3)	The relationship between wavelength and size	Type of substrate	Decoupling method	Whether include 5G
[4]	$95 \times 60 \times 0.8$	1.33λ	FR4	Use the parasitic elements	No
[7]	$136 \times 68 \times 1$	4.37λ	FR4	Use the short neutral line	Yes
[11]	$54 \times 30 \times 1.6$	2.18λ	FR4	Use a defected ground structure	No
Proposed antenna	$23 \times 19 \times 0.406$	0.68λ	Rogers 4003C	Use SRRs to prevent electromagnetic wave propagation	Yes

has a more compact size. And it can cover 5G frequency bands very well.

4. Conclusions

A compact 5G MIMO antenna with SRRs has been proposed in this paper. Two-element microstrip MIMO antenna with two different sizes of SRRs is studied. Improvement in the antenna mutual coupling has been achieved using this method. The studied indicate that the mutual coupling in the MIMO antenna loaded by SRRs is suppressed effectively, and the improved MIMO antenna has a better performance. The simulated and measured results show a well agreement. It verifies the good performance of the MIMO antenna. The isolation between the antenna elements is better than -25 dB over all required frequency bands. This simple, compact, low-cost design makes it suitable for applications such as mobile phone terminals for the fifth generation of mobile communications.

Data Availability

The dimension parameters of proposed structure data used to support the findings of this study are included in the article. The dimension parameters of the proposed structure are presented in Figure 1 and Table 1.

Conflicts of Interest

The authors declare that they have no conflicts of interest.

Acknowledgments

This work was supported by the National Natural Science Foundation of China (no. 41704176, 41574131), the National Key Research and Development Program of China (no. 2017YFF0105704), and the Fundamental Research Funds for the Central Universities from China.

References

[1] I. B. Magdău et al., "Five disruptive technology directions for 5G," *Applied Physics Letters*, vol. 12, no. 7, pp. 87–94, 2015.

[2] G. J. Foschini and M. J. Gans, "On limits of wireless communications in a fading environment when using multiple antennas," *Wireless Personal Communications*, vol. 6, no. 3, pp. 311–335, 1998.

[3] B. N. Getu and J. B. Andersen, "The MIMO cube - A compact MIMO antenna," *IEEE Transactions on Wireless Communications*, vol. 4, no. 3, pp. 1136–1141, 2005.

[4] Z. Li, Z. Du, M. Takahashi, K. Saito, and K. Ito, "Reducing mutual coupling of MIMO antennas with parasitic elements for mobile terminals," *IEEE Transactions on Antennas and Propagation*, vol. 60, no. 2, pp. 473–481, 2012.

[5] X. Yang, Y. Liu, Y.-X. Xu, and S.-X. Gong, "Isolation enhancement in patch antenna array with fractal UC-EBG structure and cross slot," *IEEE Antennas and Wireless Propagation Letters*, vol. 16, no. 99, pp. 2175–2178, 2017.

[6] V. Ionescu, M. Hnatiuc, and A. Topală, "Optimal design of mushroom-like EBG structures for antenna mutual coupling reduction in 2.4 GHz ISM band," in *Proceedings of the 5th IEEE International Conference on E-Health and Bioengineering, EHB 2015*, Iasi, Romania, November 2015.

[7] X. Shi, M. Zhang, S. Xu, D. Liu, H. Wen, and J. Wang, "Dual-band 8-element MIMO antenna with short neutral line for 5G mobile handset," in *Proceedings of the 2017 11th European Conference on Antennas and Propagation (EUCAP)*, pp. 3140–3142, Paris, France, March 2017.

[8] S. Zhang and G. F. Pedersen, "Mutual coupling reduction for UWB MIMO antennas with a wideband neutralization line," *IEEE Antennas and Wireless Propagation Letters*, vol. 15, pp. 166–169, 2016.

[9] A. Habashi, J. Nourinia, and C. Ghobadi, "A rectangular defected ground structure (DGS) for reduction of mutual coupling between closely-spaced microstrip antennas," in *Proceedings of the 20th Iranian Conference on Electrical Engineering (ICEE '12)*, pp. 1347–1350, IEEE, Tehran, Iran, May 2012.

[10] M. I. Ahmed, A. Sebak, E. A. Abdallah, and H. Elhennawy, "Mutual coupling reduction using defected ground structure (DGS) for array applications," in *Proceedings of the 15th International Symposium on Antenna Technology and Applied Electromagnetics (ANTEM '12)*, pp. 1–5, IEEE, Toulouse, France, June 2012.

[11] A. A. Ibrahim, M. A. Abdalla, A. B. Abdel-Rahman, and H. F. A. Hamed, "Compact MIMO antenna with optimized mutual coupling reduction using DGS," *International Journal of Microwave and Wireless Technologies*, vol. 6, no. 2, pp. 173–180, 2014.

[12] M. Farahani, J. Pourahmadazar, M. Akbari, M. Nedil, A. R. Sebak, and T. A. Denidni, "Mutual coupling reduction in millimeter-wave MIMO antenna array using a metamaterial polarization-rotator wall," *IEEE Antennas and Wireless Propagation Letters*, vol. 16, pp. 2324–2327, 2017.

[13] Q. Zhang, Y. Jin, J. Feng, X. Lv, and L. Si, "Mutual coupling reduction of microstrip antenna array using metamaterial absorber," in *Proceedings of the 2015 IEEE MTT-S International Microwave Workshop Series on Advanced Materials and Processes for RF and THz Applications (IMWS-AMP)*, pp. 1–3, Suzhou, China, July 2015.

[14] I. Gil and R. Fernandez-Garcia, "Study of metamaterial resonators for decoupling of a MIMO-PIFA system," in *Proceedings of the 2016 International Symposium on Electromagnetic Compatibility, EMC EUROPE*, pp. 552–556, Wroclaw, Poland, September 2016.

[15] S. Blanch, J. Romeu, and I. Corbella, "Exact representation of antenna system diversity performance from input parameter description," *Frequenz*, vol. 39, no. 9, pp. 705–707, 2003.